J Porous Mater (2012) 19:641–647
DOI 10.1007/s10934-011-9515-4

Synthesis, characterization and catalytic application of mesoporous molecular sieves SBA-15 functionalized with phosphoric acid

Baoping Wu · Zhiwei Tong · Xingdong Yuan

Published online: 4 September 2011

Abstract The phosphoric acid groups has been successfully grafted on the surface of mesoporous molecular sieve SBA-15 to form a solid acid catalyst P-SBA-15 by post-synthesis method. The samples were characterized by means of XRD, FT-IR, SEM, TEM, ^{31}P MAS NMR, NH_3-TPD, N_2 adsorption/desorption and the esterification reaction. The XRD and N_2 adsorption/desorption results indicate that P-SBA-15 catalyst keeps the 2D hexagonal mesoporous structure and opens channels with the lower surface area of 554.35 m^2/g compared with that of SBA-15. The SEM and TEM results show that the figuration of P-SBA-15 behaves "rod-like" and phosphoric acid groups is scattered differently on the surface of P-SBA-15. The FT-IR and ^{31}P MAS NMR results display that phosphorus species graft onto the surface of SBA-15, which provide the Brønsted acid sites on the surface of P-SBA-15. The acidity of the generated Brønsted acid sites on P-SBA-15 significantly is verified by NH_3-TPD. The esterification reaction results shows that catalytic activity of P-SBA-15 is enhanced significantly compared with that of SBA-15, and its stability is good.

Keywords Mesoporous molecular sieve · SBA-15 · Phosphoric acid groups · Esterification

B. Wu (✉) · Z. Tong
Department of Chemical Engineering, Huaihai Institute of Technology, Lianyungang 222005, Jiangsu, People's Republic of China
e-mail: wbp1006@yahoo.com.cn

X. Yuan
School of Petrochemical Engineering, Liaoning University of Petroleum and Chemical Technology, Fushun 113001, Liaoning, People's Republic of China

1 Introduction

Currently, there is a great interest in the esterification reaction because organic esters are frequently used in the production of plastic derivatives, perfumery, agro-chemistry and other branches of fine chemistry [1, 2]. Esterification reaction is typical acid-catalyzed reaction, which is traditionally carried out in the homogeneous phase using mineral acid catalysts (H_2SO_4, HCl, et al.) [3]. However, mineral acid catalysts are corrosive, non-recyclable and need to be neutralized for disposal after the reaction. Hence, heterogeneous solid acid catalyst has been widely investigated as being a more viable industrial process than homogeneous catalysis in producing organic esters. Compared with homogeneous acid catalysts, Heterogeneous solid acid catalysts have the advantages of lower toxicity, catalyst recovery and recyclability, minimized corrosion capacity, ease of handling and separation from the reaction medium; for these reasons, they are often called "environmental friendly catalysts" [4–8].

In recent years, mesoporous materials MCM-41 functionalized with organic–inorganic acids to obtain heterogeneous solid acid catalyst have been widely studied [9–11]. However, the lower thermal stability and hydrothermal stability have been greatly limited its practical applications in comparison with commercial zeolite catalysts [12–15]. Fortunately, the mesoporous molecular sieve SBA-15 was synthesized by Zhao et al. in 1998 [16, 17]. The mesoporous materials SBA-15 with a large pore size (4–30 nm) and thick pore wall (3–6 nm) keeps higher thermal and hydrothermal stability than MCM-41 for the acid-catalyzed reactions. The most widely used strategies to functionalize the mesoporous silica materials are the direct-synthesis process (one-pot synthetic approach) and the post-synthesis method (two-step synthetic approach). Ling et al.

[18] reported that SBA-15 functionalized with aryl sulfonaic acid groups by direct-synthesis process is efficient for the esterification of ethanol with aliphatic acid. Pitchumani et al. [19] synthesized SBA-15 selectively using a weak acid H_3PO_4 instead of the strong acid HCl by a direct-synthesis approach, their results show that the presence of phosphorus in calcined samples might provide additional Brønsted acid sites for potential applications in catalysis. However, the functionalized mesoporous silica by direct-synthesis process may induce a lower hydrothermal stability compared with that by the post-synthesis method [20]. Besides, both the internal and external surfaces of SBA-15 covered with many silanol groups offer new opportunities for the design and synthesis of novel solid catalysts by post-synthesis method.

In this work, the mesoporous molecular sieve SBA-15 was functionalized with phosphoric acid by post-synthesis method to obtain a novel solid acid catalyst having high specific area, high thermal stability and catalytic activity for the esterification reaction. The textural properties of the obtained catalyst P-SBA-15 were characterized by X-ray diffraction (XRD), N_2 adsorption/desorption (BET), transmission electron microscopy (TEM). The phosphorus species grafted onto the surface of SBA-15 and the Brønsted acid sites on P-SBA-15 were studied by fourier transform infrared (FT-IR), ^{31}P nuclear magnetic resonance (^{31}P MAS NMR). The number and the acidity of the generated Brønsted acid sites on P-SBA-15 were examined by temperature programmed desorption of ammonia (NH_3-TPD). The catalytic activity and stability of P-SBA-15 were investigated by the esterification reaction of citric acid with butanol.

2 Experimental

2.1 Sample preparation

The pure silica SBA-15, used as a catalyst support, was prepared according to the following procedure. 2 g of Pluronic P123 triblock polymer ($EO_{20}PO_{70}EO_{20}$, $Mav = 5800$, Aldrich) as the template was dissolved in 45.6 g of deionized water and 12.6 g (37%, wt%) of HCl at room temperature. After stirring for 4 h, 4.4 g of tetraethylorthosilicate (TEOS, Aldrich) as the siliceous source was added. This mixture was continuously stirred at 40 °C for 5 h, and then crystallized at 100 °C for 24 h in a Teflon-lined autoclave. The solid product was separated by filtration, washed with distilled water and dried at 100 °C in an air over night. Finally, the sample was calcined in an air at 550 °C with a heating rate of 1 °C/min and isothermal period of 5 h to decompose the structure-directing agent and the obtained white solid powder was denoted as SBA-15.

The containing phosphoric acid groups material was prepared by post-synthesis route. 2 g of calcined SBA-15 and 0.92 g of H_3PO_4 were added to 50 g of acetone solvent. The obtained suspension (P/Si = 0.07, the molecular weight of SBA-15 regard as SiO_2) was stirred at room temperature. Then, the acetone was evaporated at 60 °C under stirring. The functionalized SBA-15 sample was calcined at 500 °C for 4 h, and the resultant powder was denoted as P-SBA-15.

2.2 Catalyst characterization

The X-ray diffraction (XRD) patterns were recorded on Scintag XRS200 diffractometer using Cu-Kα radiation (30 kV and 100 mA). The scanning 2θ range was from 0.7° to 5°, scanning speed of 0.1°/min. Nitrogen adsorption/desorption isotherms were measured at 77 K using Quantachrome Auto-Sorb-1 Analyzer. Prior to the measurements, the samples were degassed at 537 K for 3 h. The specific surface area was performed according to the B.E.T method. The pore size distribution curves were calculated from the adsorption branches of the isotherms using B.J.H approach. The Fourier transform infrared (FT-IR) spectra of samples were recorded as KBr in the wavenumber region of 2,000–400 cm^{-1} with a Nicolet 5Dx-FTIR spectrometer. Transmission electron microscopy (TEM) was performed using a JEM-2010 at an acceleration voltage of 120 kV. Scanning electron microscopy (SEM) was taken on an Hitachi S-800 with an acceleration voltage of 5 kV. The samples were coated with platinum before the measurements in order to avoid the charge effect. ^{31}P MAS NMR spectra were obtained at 202.45 MHz on an Infinity Plus 300WB NMR spectrometer with a 5 mm solid MAS probe by using 85% H_3PO_4 as the internal standard. Temperature programmed desorption of ammonia (NH_3-TPD) was performed in a quartz micro-reactor. 0.10 g of sample was firstly loaded in the reactor and heated in flowing He at 773 K for 2 h. NH_3 was then introduced to the reactor after it was cooled down to room temperature. To remove the weakly adsorbed NH_3, the sample was swept using flowing He at 373 K for 2 h. The TPD experiments were then carried out in flowing He from 373 to 1073 K at a linear heating rate of 10 °C min^{-1}.

2.3 Catalytic testing

The P-SBA-15 sample was tested as catalyst for the esterification of citric acid and butanol. The catalytic experiments were directly performed in a 100 mL regular glass reactor with magnetic stirrer, heated in an oil bath at atmospheric pressure. The reactant was analyzed by HP4890 gas chromatograph using FID detector with a capillary column of OV-101 (Φ 0.25 mm × 30 m).

3 Results and discussion

3.1 XRD

Figure 1 shows the low-angle X-ray diffraction patterns of the pure silica SBA-15 (Fig. 1a) and P-SBA-15 (Fig. 1b) samples. As can be seen from Fig. 1a, an intensive peak at $2\theta = 0.82°$ corresponding to the (100) diffraction peak, accompanying with two small peaks assigned to (110) and (200) diffraction peaks, is characteristic of the ordered mesopore structure of 2D hexagonal space group (p6 mm) [16, 21]. For the P-SBA-15 sample, the three diffraction peaks indicate that the hexagonal mesoporous structure have been retained after phosphoric acid treatment. However, the intensity of the diffraction peaks for P-SBA-15 decreases, which may be caused by the different scattering phosphoric acid groups on the surface of SBA-15; as a result, the mesopore structure of P-SBA-15 becomes less ordered than that of SBA-15.

3.2 SEM and TEM

In the catalysts preparing process, it is very important to keep the active ingredients highly dispersed in pore channels of the mesoporous matrix and remain pore channel open to reactants. SEM images of SBA-15 and P-SBA-15 samples are shown in Fig. 2. The figuration of SBA-15 behaves "rod-like" (Fig. 2a). After grafted phosphoric acid groups, the "rod-shape" of P-SBA-15 becomes shorter and thinner (Fig. 2b).

The pore shape and pore distribution of SBA-15 [including different orientations: electron beam parallel to the channel (Fig. 3a) and electron beam vertical to the channel (Fig. 3b)] can be obviously observed in TEM,

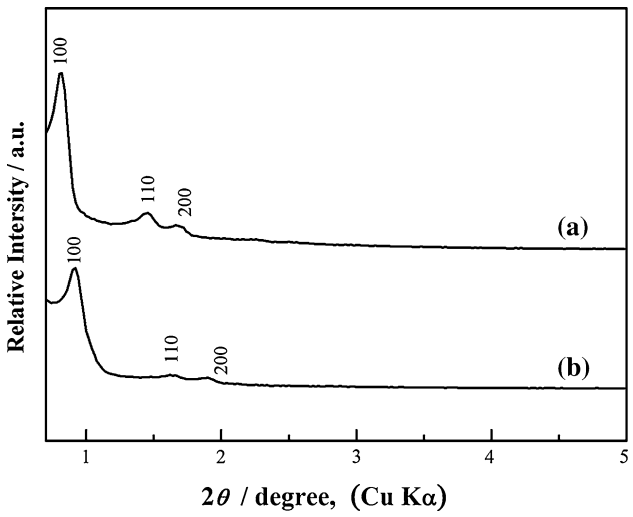

Fig. 1 XRD patterns of samples SBA-15 (**a**) and P-SBA-15 (**b**)

which indicate the highly ordered two-dimensional hexagonal mesoporous structure. After grafted phosphoric acid groups, the electron beam parallel to the pore channels; small bulk of the phosphorus acid, i.e. the black parts aggregating on the outer surface, could be found (Fig. 3c). The order of pore distribution of P-SBA-15 decreases compared with that of SBA-15, while its pore shape remains the hexagonal mesostructure with the electron beam vertical to the channel (Fig. 3d).

3.3 BET

Figure 4 shows the nitrogen adsorption/desorption isotherms of the pure silica SBA-15 (Fig. 4a) and P-SBA-15 (Fig. 4b) samples. The samples are found to be of typical type IV isotherms with a H1 hysteresis loop [16, 22]. Furthermore, the P/P_0 position of the inflection points is related to a diameter in the mesoporous range, and the sharpness of these steps indicates the uniformity of the pore size. It can be seen clearly that the P/P_0 position for P-SBA-15 shifts to lower value compared with that of SBA-15, which may imply that phosphoric acid groups loaded makes the pore size of SBA-15 become smaller. The sharpness of these steps for P-SBA-15 remain invariable which indicates that the P-SBA-15 has the uniform pore size. The same results are shown in the BJH pore size distribution curves (Fig. 5). From Fig. 5, the pore size distribution curves of samples shows very narrow peaks with a maximum at about 7.0 nm, which indicates the uniformity of the pores for the materials. Furthermore, the narrow pore size distribution curve, the high BET surface area, mean pore size and pore volume plus the distinct X-ray reflection peaks demonstrate that the P-SBA-15 has a hexagonal mesoporous structure.

The structural parameters of SBA-15 and P-SBA-15 are given in Table 1. The structural parameters of SBA-15 show surface area of 678.30 m^2/g, pore volume of 0.97 cm^3/g, and mean pore size of 7.13 nm. Phosphoric acid groups grafted onto the surface of SBA-15 results in the decrease of some structural parameters values. Thus, BET surface area decreases to 554.35 m^2/g, pore volume to 0.87 cm^3/g, and mean pore size to 6.07 nm. But P-SBA-15 remains the characteristic mesoporous structure.

3.4 FT-IR

The FT-IR spectra of SBA-15 and P-SBA-15 are displayed in Fig. 6. All materials exhibited a broad intense signal in the 1300–1,000 cm^{-1} region corresponding to the characteristic Si–O–Si stretch adsorption [23–26]. In addition to the peaks observed in the FT-IR spectrum of SBA-15, the P-SBA-15 exhibited the new bands at 536 and 609 cm^{-1}, which corresponded to P–O stretching, O = P–O bending

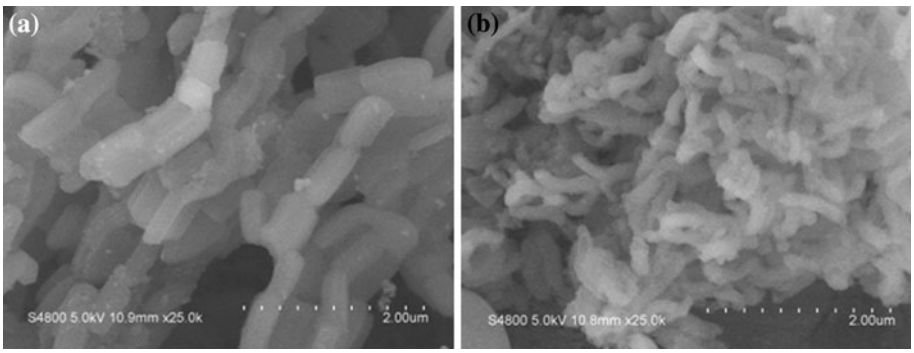

Fig. 2 SEM images of the pure silica SBA-15 (**a**) and P-SBA-15 (**b**)

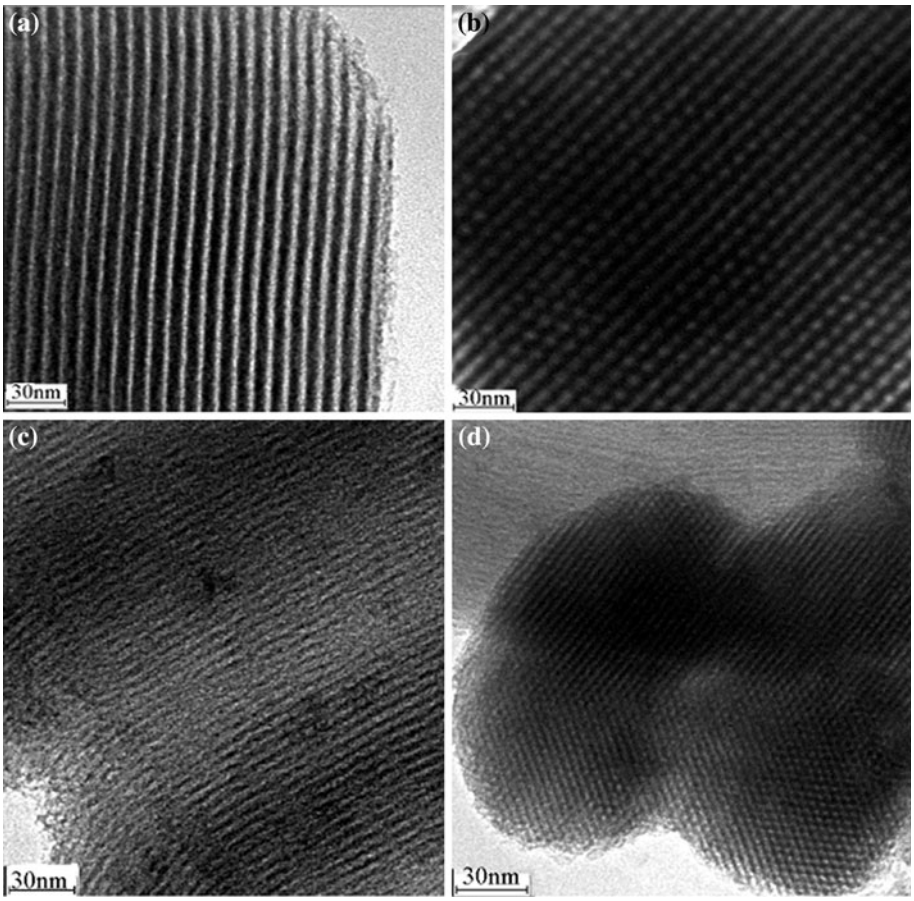

Fig. 3 TEM photographs of SBA-15 (**a**, **b**) and P-SBA-15 (**c**, **d**): **a** and **c** in the direction parallel to pore axis; **b** and **d** in the direction perpendicular to the pore axis

and O–P–O bending mode of vibration, respectively [27]. The FT-IR spectra results suggest the existence of phosphate groups in the sample P-SBA-15. The composition of P-SBA-15 was also further confirmed by the ^{31}P MAS NMR spectrum.

3.5 ^{31}P MAS NMR

The mechanism of grafted phosphoric acid groups onto the surface of SBA-15 may be the dehydration reaction between the hydroxyl groups of H_3PO_4 and surface isolated −OH groups of SBA-15. After high temperature calcination, P(OSi) bond or $P(OSi)_2$ bond may form by the dehydration of one or two water molecule, which grafts the phosphoric acid groups onto the surface of SBA-15. Although the hydroxyl groups of phosphoric acid can be removed by dehydration during high temperature calcination, the hydroxyl groups can be restored after adsorption of moisture from the air. These restored hydroxyl groups on phosphoric acid have the ability to donate protons, which may produce Brønsted acid sites on the surface of SBA-15 and improve its overall acidity. Thus, the phosphoric acid functionalized SBA-15 may be used as a promising catalyst for specific reactions.

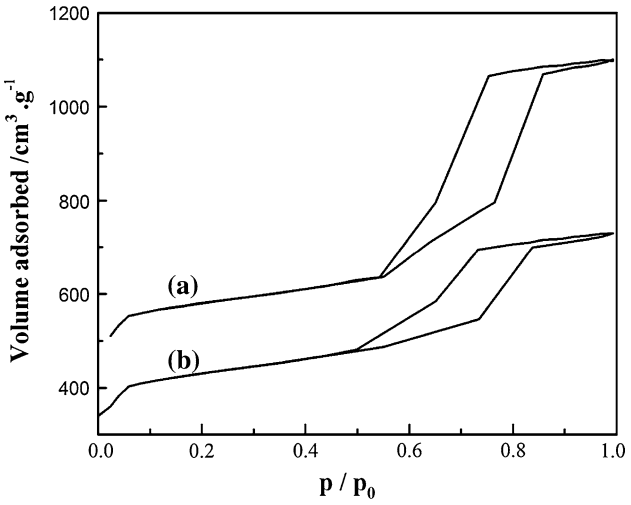

Fig. 4 Nitrogen adsorption/desorption isotherms of SBA-15 (**a**) and P-SBA-15 (**b**)

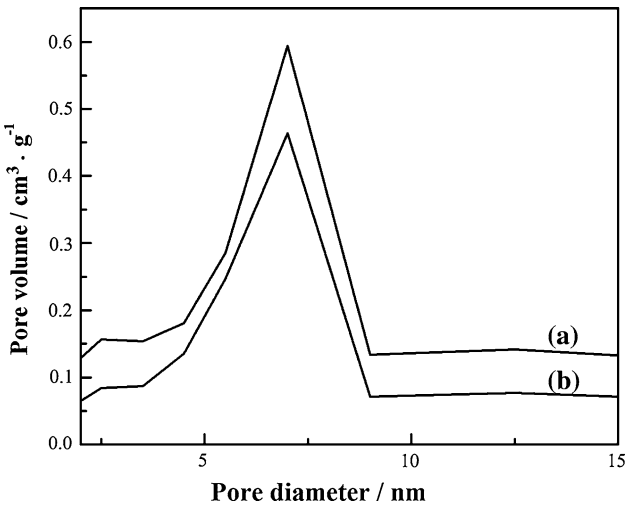

Fig. 5 The pore size distribution curves of SBA-15 (**a**) and P-SBA-15 (**b**)

The ^{31}P MAS NMR spectra of the P-SBA-15 (Fig. 7) was measured by Infinity Plus 300WB NMR spectra-meter in order to testify grafted phosphoric acid groups on the surface of SBA-15. As can be seen from Fig. 7a, the result illustrates that the ^{31}P MAS NMR spectrum of sample P-SBA-15 before calcination consists of three resonance peaks. Besides the peak at 0 ppm corresponding to H_3PO_4, additional resonances are present at ca. −11 and −47 ppm,

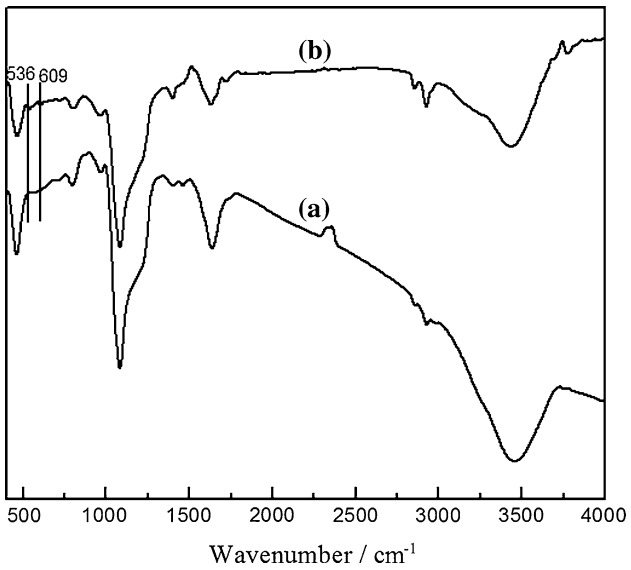

Fig. 6 The FT-IR spectra of SBA-15 (**a**) and P-SBA-15 (**b**)

which are assigned to P(OSi) and intermediate P_4O_{10} groups, respectively. As can be see from Fig. 7b, the −47 ppm resonance peak disappears and −11 ppm resonance peak exist, which indicates that dehydration reaction between the hydroxyl groups of H_3PO_4 and surface isolated −OH groups of SBA-15 happen to form P(OSi) groups on the surface of SBA-15. The resonance peaks at −25 and −35 ppm assigned to $P(OSi)_2$ bond and $P(OSi)_3$ bond have not been found, which reveals that hydroxyl groups of H_3PO_4 do not integrate with two or three of the SBA-15 surface isolated −OH groups [28–32]. According to the mechanism of grafted phosphoric acid groups onto the surface of SBA-15, many P(OSi) groups on the surface of SBA-15 have the ability to donate protons, which may produce Brønsted acid sites on the surface of SBA-15 to obtain solid acid catalyst P-SBA-15.

The signals of atom P in the 30–40 ppm region have been attributed to the formation of Lewis acid sites by the substitution of framework Si atoms of SBA-15 with P atoms of H_3PO_4 [29, 33]. However, the ^{31}P MAS NMR spectrum of P-SBA-15 sample has no resonance peaks in the 30–40 ppm region, which indicates that no Lewis acid sites exist on the surface of P-SBA-15.

Thus it can be seen, the existence of phosphate groups in the sample P-SBA-15 was determined by FT-IR, and Brønsted acid sites on the surface of SBA-15 was examined

Table 1 Structure parameters for SBA-15 and P-SBA-15

Samples	d_{100} (nm)	a_0 (nm)	A_{BET} (m^2/g)	v_{BJH} (cm^3/g)	d_{pore} (nm)
SBA-15	11.03	12.74	678.30	0.97	7.13
P-SBA-15	9.57	11.50	554.35	0.87	6.07

$d = \lambda/2\sin\theta$, $a_0 = 2\ d_{100}/(3)^{1/2}$

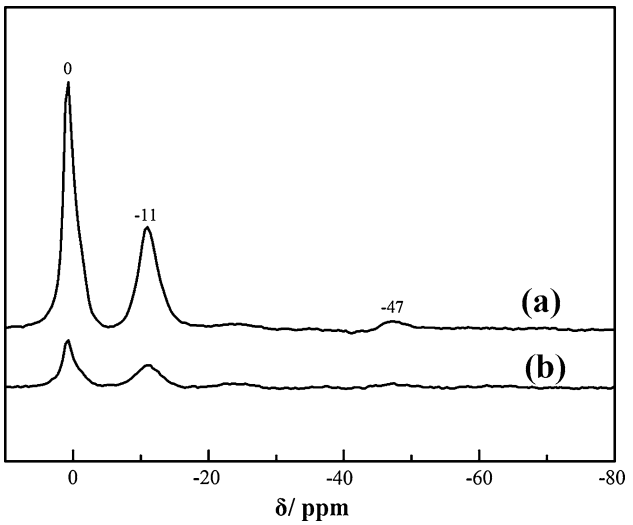

Fig. 7 The ^{31}P MAS NMR spectra of P-SBA-15 **a** before calcined sample; **b** after calcined sample

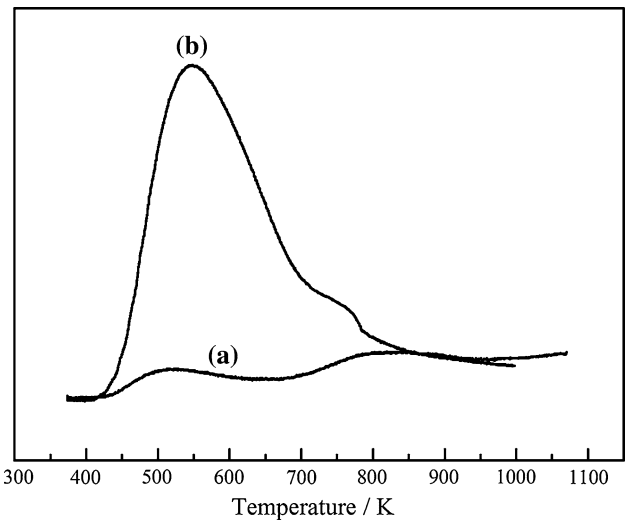

Fig. 8 The NH_3-TPD of SBA-15 and P-SBA-15 samples

by ^{31}P MAS NMR, which show that the solid acid catalyst P-SBA-15 having Brønsted acid sites has been successfully by the post-synthesis method. At the same time, the number and the activity of the Brønsted acid sites on P-SBA-15 was further studied by NH_3-TPD.

3.6 NH_3-TPD

The number and strength of the Brønsted acid sites over P-SBA-15 was further studied by the temperature programmed desorption of ammonia (NH_3-TPD). Figure 8 shows the desorption profile of NH_3 from SBA-15 and P-SBA-15 samples. There is a very small amount of desorption of NH_3 from SBA-15 as it lacks acid sites. However, the amount of NH_3 desorbed from the P-SBA-15 sample is substantial, indicating that the number of Brønsted acid sites on P-SBA-15 can be substantially increased by simply grafting the phosphorus species onto its surface.

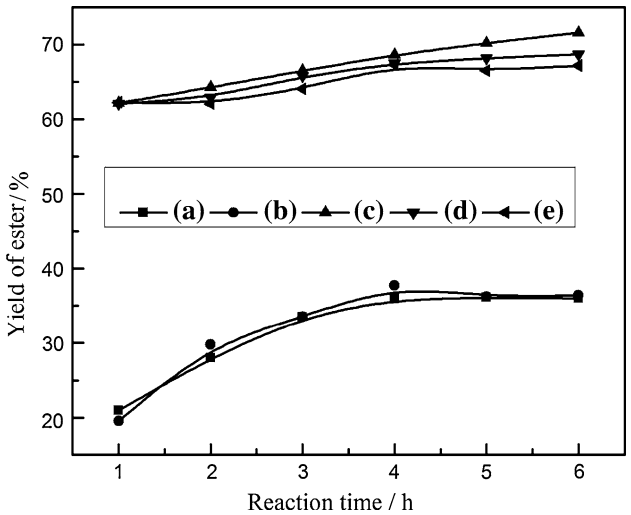

Fig. 9 The catalytic activity and stability test of P-SBA-15 catalyst on the esterfication of citric acid. **a** no catalyst; **b** SBA-15; **c** P-SBA-15 (1st run); **d** P-SBA-15 (2nd run); **e** P-SBA-15 (3rd run). Reaction condition: react temperature = 140 °C, the molar ratio citric acid and butanol = 1:6, the mass ratio of catalyst to reactant = 1.5%

3.7 Catalyst evaluation

The catalytic performance and stability of P-SBA-15 were evaluated by esterification of citric acid with butanol (Fig. 9), the experiments including no catalyst and the pure silica SBA-15 were investigated in contrast. While the reaction was carried out for 6 h, little difference in the yield of tributyl citrate can be observed between SBA-15 catalyst addition and no catalyst addition experiments; which indicates that SBA-15 has little catalytic activity for this reaction. P-SBA-15 shows high catalytic activity which implies the phosphoric acid groups are the active centers for esterification reaction. The stability of catalyst P-SBA-15 shows that the yield of tributyl citrate is basically invariable from the first run to the third run. The P-SBA-15 is efficient mesoporous solid acid catalyst for the esterification reaction of citric acid and butanol.

4 Conclusions

The mesoporous molecular sieve SBA-15 functionalized with phosphoric acid groups (P-SBA-15) was synthesized by post-synthesis method. The structure of P-SBA-15 catalyst remains the typical hexagonal array structure of the pure silica SBA-15 confirmed by XRD, TEM, and SEM

measurement. The XRD results show that the intensity of the diffraction peaks for P-SBA-15 decrease, which is attributed to loading phosphoric acid groups on the surface of SBA-15. This is in accordance with the results of SEM and TEM. The nitrogen adsorption/desorption isotherms of P-SBA-15 samples are Type IV in nature and exhibit a H1 hysteresis loop with surface area of 554.35 m^2/g, pore volume of 0.87 cm^3/g and mean pore size of 6.07 nm. The ^{31}P MAS NMR and FT-IR results testify phosphoric acid groups grafted onto the surface of SBA-15, and the obtained catalyst P-SBA-15 has Brønsted acid sites. There is a very small amount of desorption of NH_3 from SBA-15, while the large amount of NH_3 desorbed from the P-SBA-15 sample is confirmed by NH_3-TPD. The catalytic properties of P-SBA-15 are evaluated by the esterification of citric acid and butanol, the result shows that the P-SBA-15 catalyst exhibits well catalytic activity and stability for the esterification.

Acknowledgments This work was supported by a Grant-in-aid for Scientific Research from the Japan Society for the Promotion of Science (JSPS) and the CREST program of the Japan Science and Technology Agency (JST). We are grateful to young and middle aged academic leaders of Jiangsu Province universities' "blue and green blue project". This work is also supported by National Natural Science Foundation of China (Grant No. 50873042).

References

1. K.C. Wu, Y.W. Chen, Appl. Catal. Gen. **257**, 33 (2004)
2. Y. Liu, E. Lotero, J. Catal. **243**, 221 (2006)
3. J.M. Marchetti, A.F. Errazu, Biomass Bioenergy **32**, 892 (2008)
4. J.H. Clark, Acc. Chem. Res. **35**, 791 (2002)
5. T.S. Thorat, V.M. Yadav, G.D. Yadav, Appl. Catal. A Gen. **90**, 73 (1992)
6. Y. Liu, E. Lotero, J.G. Goodwin, J. Mol. Catal. A Chem. **245**, 132 (2006)
7. G.D. Yadav, M.B. Thathagar, React. Funct. Polym. **52**, 99 (2002)
8. S. Ramu, N. Lingaiah, B.L.A. Prabhavathi Devi, R.B.N. Prasad, I. Suryanarayana, P.S. Sai Prasad, Appl. Catal. A Gen. **276**, 163 (2004)
9. S.J. Miao, B.H. Shanks, Appl. Catal. **395**, 113 (2009)
10. W.D. Bossaert, D.E. De Vos, W.M. Van Rhijn, J. Bullen, P.J. Grobet, P. Jacobs, J. Catal. **182**, 156 (1999)
11. I. Diaz, F. Mohino, J. Perez-Pariente, E. Sastre, Appl. Catal. A Gen. **205**, 19 (2001)
12. R. Ryoo, S. Jun, J. Phys. Chem. **101**, 317 (1997)
13. S. Inagaki, Y. Sakamoto, Y. Fukushima, O. Terasaki, Chem. Mater. **8**, 2089 (1996)
14. D. Coutinho, A.O. Acevedo, G.R. Dieckmann, K.J. Balkus Jr., Micropor. Mesopor. Mater. **54**, 249 (2002)
15. N.N. Trukhan, V.N. Romannikov, A.N. Shmakov, M.P. Vanina, E.A. Paukshtis, V.I. Bukhtiyarov, V.V. Kriventsov, I.Y. Danilov, O.A. Kholdeeva, Micropor. Mesopor. Mater. **59**, 73 (2003)
16. D.Y. Zhao, J. Feng, Q. Huo, N. Melosh, G.H. Fredickson, B.F. Chmelka, G.D. Stucky, Science **279**, 548 (1998)
17. D.Y. Zhao, Q.S. Huo, J.L. Feng, B.F. Chmelka, G.D. Stucky, J. Am. Chem. Soc. **120**, 6024 (1998)
18. C.M. Li, J. Yang, X. Shi, J. Liu, Q.H. Yang, Micropor. Mesopor. Mater. **98**, 220 (2007)
19. R. Pitchumani, W.J. Li, M.-O. Coppens, Catal. Today **105**, 618 (2005)
20. G. Nuria, B. Esperanza, G. Julio, T. Pilar, M. Victoria, A.G. Rafael, Micropor. Mesopor. Mater. **106**, 129 (2007)
21. Y.-J. Han, J.M. Kim, G.D. Stucky, Chem. Mater. **12**, 2068 (2000)
22. M. Thommesa, R. Kohn, M. Frob, Appl. Sur. Sci. **196**, 239 (2002)
23. M.S. Wong, H.C. Huang, J.Y. Ying, Chem. Mater. **14**, 1961 (2002)
24. B.L. Newalkar, J. Olanrewaju, S. Komarneni, Chem. Mater. **13**, 552 (2001)
25. B. Chakraborty, B. Viswanathan, Catal. Today **49**, 253 (1999)
26. Z.H. Luan, E.M. Maes, A.W. Paul, V.D. Heide, D.Y. Zhao, R.S. Czernuszewicz, L. Kevan, Chem. Mater. **11**, 3680 (1999)
27. K. Rajesh, P. Mukundan, P.K. Pillai, V.R. Nair, K.G.K. Warrier, Chem. Mater. **16**, 2700 (2004)
28. C. Coelho, T. Azaïs, L. Bonhomme-Coury, J. Maquet, C. Bonhomme, C.R. Chimie. **9**, 472 (2006)
29. T. Blasco, A. Corma, J. Martínez-Triguero, J. Catal. **237**, 267 (2006)
30. T.A. Zepeda, B. Pawelec, J.L.G. Fierro, A. Montesinos, A. Olivas, S. Fuentes, T. Halachev, Micropor. Mesopor. Mater. **111**, 493 (2008)
31. Z.M. Yan, B.T. Chen, Y.N. Huang, Solid State Nucl. Magn. Reson. **35**, 49 (2009)
32. K.U. Nandhini, B. Arabindoo, M. Palanichamy, V. Murugesan, J. Mol. Catal. A Chem. **243**, 183 (2006)
33. J. Guan, X.J. Li, G. Yang, J. Mol. Catal. A. Chem. **310**, 113 (2009)